31st Annual International Conference of the IEEE EMBS
Minneapolis, Minnesota, USA, September 2-6, 2009

A Pulse Simulator for Crystal Identification Validation of *Phoswich* Detectors used in Positron Emission Tomography

H. Camilia Yousefzadeh, *Student Member, IEEE*, Roger Lecomte, *Member, IEEE,* and Réjean Fontaine, *Senior*, *IEEE*

***Abstract*— Crystal identification (CI) of *phoswich* detectors is a technique used in positron emission tomography (PET) for improving spatial resolution through depth-of-interaction determination or higher pixelization. Digital algorithms using advanced digital signal processing techniques currently provide the most powerful approaches for CI of phoswich detectors made of crystals with only slightly different scintillation decay times. Such methods can be implemented in the all-digital architecture of LabPET, a small animal PET scanner developed in Sherbrooke, for fast and accurate real-time CI. In order to validate the new CI algorithms and assess their performance for different front-end electronics, a pulse generator simulator was developed to generate PET signals and investigate the effects of factors such as electronic noise, photon statistics and pulse shaping filter. The pulse generator was validated with LabPET-like pulses and CI results were compared with experimental data. The pulse simulator enables CI algorithms to be validated together with detector performance such as energy and timing resolution at an early stage of scanner design.**

I. Introduction

DEPTH of interaction (DOI) has been investigated in positron emission tomography (PET) for correcting the parallax error which jeopardizes the spatial resolution in small animal scanners [1], [2]. One of the most common techniques for DOI measurement consists in using *phoswich* detectors that are composed of small crystals with different scintillating characteristics [3]. These crystals can be identified using classical 'Pulse Shape Discrimination' (PSD) techniques [4], [5] or more powerful digital approaches based on adaptive filter theory [6]. The LabPET, a small animal PET scanner developed in Sherbrooke [7] offers a powerful platform for testing these algorithms due to its all-digital architecture. In this scanner, analog signals issued from avalanche photodiode detectors (APD) are amplified, shaped and sampled right at the output of the charge sensitive preamplifier. Further signal processing and analyses rely on real time algorithms implemented in FPGA and/or DSP. The possibility to use such powerful digital techniques for fast crystal identification (CI) is very promising for real-time processing of *phoswich* detector signals. Among CI algorithms, the recently introduced fast Wiener filter-based CI algorithm [8] that has demonstrated high performance in discriminating crystals even for low energy events resulting from Compton scatter interactions is used for validation in this paper.

Various elements of the data acquisition chain (DAQ) might influence the CI performance. Physical phenomena such as the exact energy deposited in the *phoswich* crystals, scintillation photon statistics and APD multiplication noise all play a role in CI results. As the design of such digital CI algorithms is not actually considered as a criterion for PET electronics design, it is therefore crucial to be able to validate the performance of such algorithms as a function of these factors before its implementation in a PET scanner.

This paper reports the design of a pulse generator that mimics the behavior of the *phoswich* detectors used in the LabPET, including all noise contributions in the DAQ chain. The Geant4 Application for Tomography Emission (GATE) was used to generate energy and timing of a radiation events including inter-crystal Compton scatter in a *phoswich* detector. Using this information, artificial digital pulses are generated at a high sampling rate. Crystal and shaping model parameters as well as all noise contributions, such as statistical and electronic noise, are included in each pulse before being decimated to 45 MHz, the sampling frequency of the LabPET. The pulse generator was validated against LabPET signals. The CI algorithm performance was then evaluated under different conditions, including RC or semi-Gaussian shapers with various input noise contributions in the system.

II. Materials And Methods

Each detector in the LabPET consists of a LYSO-LGSO crystal pair (tr ~40 ns and ~70 ns, respectively), each $2 \times 2 \times \sim 12$ mm3 in size, both coupled to the same APD (gain ~80). The APD is connected to a charge sensitive preamplifier (CSP) having a gain of 1.8 mV/fC, an amplification RC integrator filter, and an anti-aliasing filter supplying the signal to an 8-bit, – 45-MHz analog to digital converter (ADC) (Fig. 1). Crystals were exposed to a 1 mCi

Manuscript received April 23, 2009. This work was supported in part by the Natural Science and Engineering Council of Canada (NSERC) and in part by Le Fonds Québécois de la Recherche sur la Nature et les Technologies (FQRNT).

H. C. Yousefzadeh, and R. Fontaine are with the Department of Electrical and Computer Engineering, Université de Sherbrooke, Québec, Canada J1K 2R1, phone: 1-819-821-8000 ext. 62783; fax: 1-819-821 7937; e-mail: h.yousefzadeh@ usherbrooke.ca.

R. Lecomte is with the Department of Nuclear Medicine and Radiobiology, Université de Sherbrooke and the Sherbrooke Molecular Imaging Center,, Sherbrooke, Québec, Canada J1H 5N4.

^{68}Ge rod source of 511 keV annihilation photons for pulse acquisition. When triggered at a user pre-set energy threshold, the digitized pulse consisting of 64 samples ($d(n)$) is stored together with its timestamp.

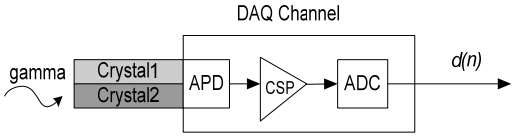

Fig. 1. The LabPET™ data acquisition chain (DAQ). A *phoswich* detector consisting of two different crystals is excited by a source of 511 keV photons; d(n) is the DAQ recorded digital output signal.

A. Fast Wiener filter-based Crystal Identification

The fast Wiener filter-based CI (WFCI) algorithm, recently developed for LabPET *phoswich* detectors was used for validation of the pulse generator [8]. Briefly, in this method a calibration process first extracts the adaptive filter pole and zero (b_0 and a_1) from 50,000 events generated by each crystal (Fig. 2a). The parameterized filter is then used as a model of each crystal (Fig. 2b). The LabPET DAQ chain model, empirically extracted and used as *a priori* known information, is incorporated into the model of each crystal and the contribution of each crystal (p_1 and p_2) in the output signal is calculated (Fig. 2b). Events are classified as LYSO or LGSO depending if the percentage p_1 is superior or inferior to a threshold of 50%, respectively.

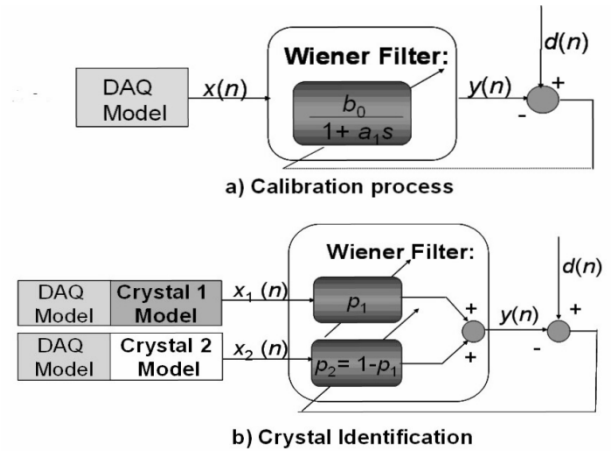

Fig. 2. a) An adaptive Wiener filter is used to extract time constant (pole) and light efficiency (zero) of each crystal in Z domain from 50,000 signals during a calibration process. $x(n)$ is the LabPET DAQ chain model as *a priori* known information, $d(n)$ is the generated signal and $y(n)$ the output signal of the Wiener filter. b) The Crystal Identification (CI) process uses the model of each crystal, $x_1(n)$ and $x_2(n)$, to extract the respective crystal contribution in each signal. This is done by calculating the percent fraction (or color) of each crystal (p_1 and p_2) in the output signal.

B. DAQ chain simulation & Noise contribution to WFCI

In this study, the LabPET *phoswich* detector was simulated in GATE under the same irradiation conditions. The time dependence of the photoelectron pulse $N(t)$ at the output of the APD can be approximated by:

$$N(t) = M \cdot Q_0 \cdot \exp(-t/\tau_s) \quad (1)$$

where Q_0 is the initial primary photoelectron yield generated in the APD (~3000 and ~2000 photoelectron per MeV for LYSO and LGSO crystals respectively) , τ_s the crystal decay time constant and M the APD gain. Scintillation pulses were generated using GATE by tracking the 511 keV interactions in the *phoswich* detectors. The shaper output pulse was generated by mathematical convolution of the crystal model described in (1) with the impulse response of the LabPET DAQ chain CSP/RC shaper, assumed to be time-invariant. At this point, noise contributions from all sources were added to the signal before digitization.

Three sources of noise are present in the system: 1) the electronic noise measured as the Equivalent Noise Charge (ENC) referred to the CSP/RC filter input, which is Gaussian and stationary [9] and estimated to be lower than 700 electrons RMS for the LabPET. The ENC noise is converted to Volt RMS (σ_{ENC}) by the CSP gain of 1.8 mV/fC before being added to the CSP output signals; 2) the photon statistical noise (σ_s) resulting from the scintillation emission process in the crystal, which follows a Poisson distribution and, in the case of the LabPET, has been evaluated as ~ 9% at the maximum point of the shaper output signal [10]; 3) the multiplication noise (σ_p) due to the electron generation in the APD which also follows a Poisson distribution as described in [11].

All noise contributions were computed using Matlab to generate LabPET-like pulses. Noise is added to each sample of the generated signal, at a frequency 32 times higher than the ADC sampling frequency. At the end, the signal is decimated at 45 MHz in phase with the timestamp extracted from GATE and 64 samples are preserved. These simulated events were found to be very similar to experimental LabPET events (Fig. 3).

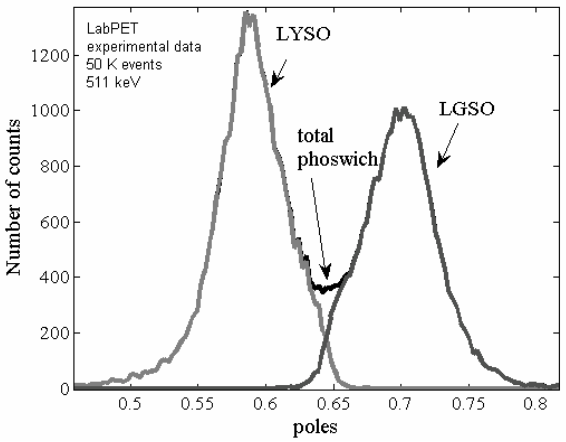

Fig. 3. The Pole spectrum of 50,000 experimental LabPET events processed using WFCI.

For each type of added noise, simulated signals were

presented to the WFCI algorithm in order to assess the performance and CI error rate of the algorithm for that type of noise. The effect of each noise source on CI error rate was assessed by feeding the simulated signals to the WFCI algorithm. CI results were compared to the actual location of interactions extracted from GATE.

C. Shaper filtering factor contributing to WFCI

Simulated data with different shaping function were generated. Contrary to the previous step where data were mimicking the LabPET pulses, here the WFCI performance was evaluated for different shapers with different time constants. An RC shaper with 1.5 µs decay times and a first order CR-RC^n shaper filter with 50 ns decay time were used instead of the LabPET shaper for data generation (Fig. 4).

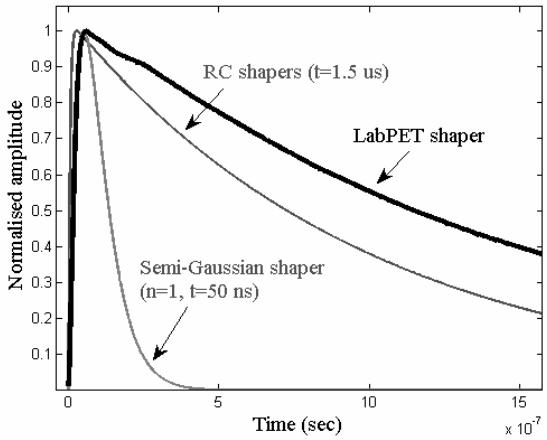

Fig. 4. An RC shaper with 1.5 µs decay times and a first order semi-Gaussian CR-RC^n shaper with 50 ns decay constant compared with the LabPET shaper.

III. RESULTS

Fig. 5 shows the contribution of the different system noise sources on the pole spectrum of 50,000 simulated events using a LabPET DAQ chain impulse response. As shown, the photon statistical noise significantly increases the spread of the peak in the pole spectrum and decreases the CI resolution. Fig. 6 shows the WFCI results. This figure is comparable to the experimental CI results of Fig. 3 that shows the pole spectrum of 50,000 LabPET experimental data. The peak widths of both pole spectra are similar, confirming that the added noise on the simulated data yields a signal-to-noise ratio that is proportional to that of the experimental data. An analysis of the influence of each type of noise on the CI error showed that the CI error rate increases from 2% for signals with only ENC noise to 5% for signals that have photon statistical noise added.

Fig. 7 shows the CI results on the pole spectrum of data simulated with an RC shaper having a decay time constant of 1.5 µs. The comparison of this spectrum with Fig. 3 reveals a slight shift of the mean pole peak positions. The CI error rate is ~4%, which shows a slight CI improvement due to the use of an ideal RC shaper. The peak width in the pole spectrum remains almost the same as with the experimental data.

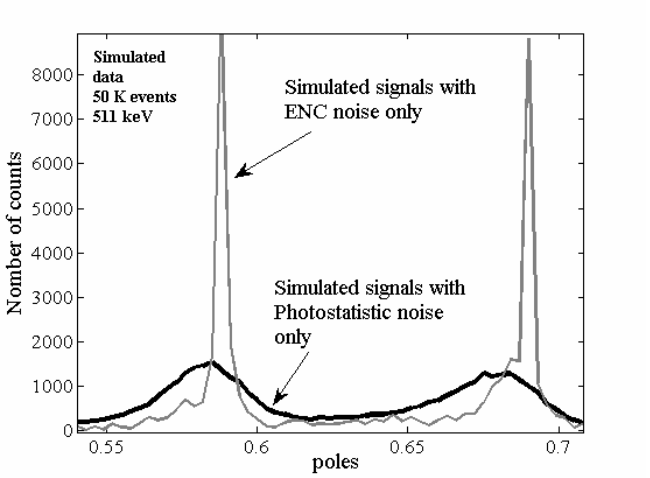

Fig. 5. Contribution of different noise sources on pole spectrum. Photon statistic noise enlarges the Gaussian curves and decreases the crystals identification performance.

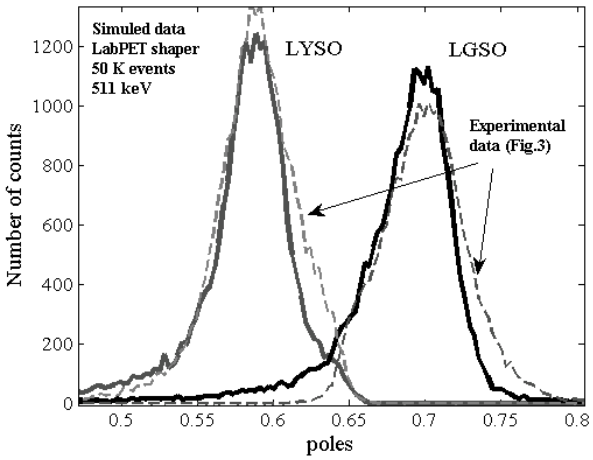

Fig. 6. Results of Wiener filter-based crystal identification (WFCI) on the pole spectrum of 50,000 simulated events using LabPET shaper.

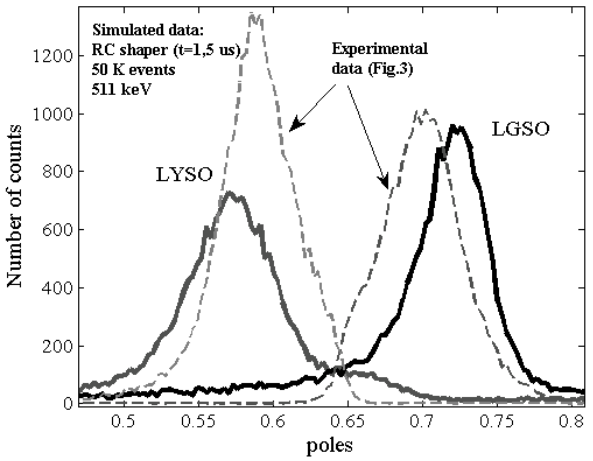

Fig. 7. Results of Wiener filter-based crystal identification (WFCI) on the pole spectrum of 50,000 simulated signals using an RC shaper with a time constant of 1.5 µs.

Fig. 8 shows CI results on the pole spectrum for signals simulated with a first order Semi-Gaussian shaper filter with 50 ns time constant (error rate 6%). The comparison of this figure with Fig. 3 shows a mean pole shift to the left.

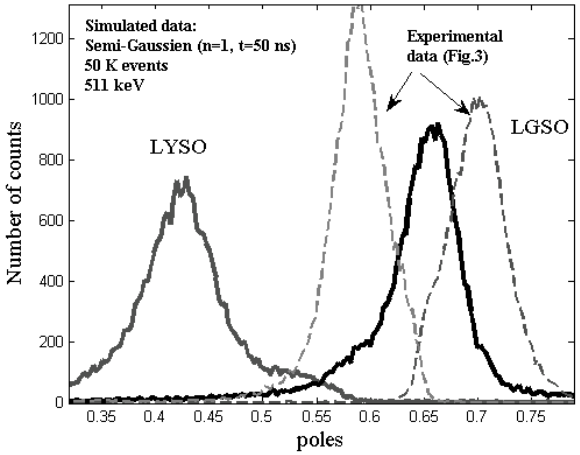

Fig. 8. Results of Wiener filter-based crystal identification (WFCI) on the pole spectrum of 50,000 simulated signals using a semi-Gaussian shaper of first order with 50 ns time constant.

IV. Discussion

In this study, a simulation pulse generator equivalent to the LabPET DAQ chain was developed. This development enabled investigation of the WFCI method [8] for different factors contributing to the performance of CI algorithm such as photon statistical noise and different shaper filters.

The Wiener filter, like other common linear time-invariant (LTI) adaptive filters, is designed to deal with white Gaussian stationary noise. Therefore, the photon statistical noise, which is a non-stationary colored Poisson process, decreases the performance of the Wiener filter algorithm. The non-white characteristic of the photon statistical noise generates uncertainties resulting in an enlargement of the peak width in the pole spectrum (Fig. 5).

It is noteworthy that the CI error rate estimated by the area extending beyond the cross point of the two peaks in the pole spectra, as used previously [8], does not represent the real CI error of the algorithm. In fact, other simulation studies (not reported here) have shown that data in the area beyond the cross point of the two peaks in the pole spectra results mainly from scatter events that have interacted in both crystals of the *phoswich* detector.

The use of various shaping filters with different time constants was shown to induce a shift in the pole spectra. However, as far as the shaper impulse response is in phase with output signals, the peak width of the pole spectrum and, consequently the error rate of the CI algorithm remained unchanged.

V. Conclusion

A pulse generator was developed to simulate PET signals and investigate the effects of various pulse shaping filters on crystal identification in PET. The simulated data were shown to achieve good agreement with experimental data, confirming the accuracy of the pulse generation process for different timing and CI algorithms. Based on the developed simulation model, the photon statistical noise was demonstrated to be the main contributor to the CI error rate, rather than the shaper filter type. As the Wiener filter algorithm is designed to deal with white Gaussian noise, its performance is affected by the non-stationary Poisson photon statistical noise. A more sophisticated algorithm such as Kalman filter or extended iterative ARMAX algorithms developed for linear time-varying systems may bring a solution to the correct estimation of this noise in real-time.

References

[1] R.S. Miyaoka, T.K. Lewellen, H. Yu, and D.L. McDanie1, "Design of a depth of interaction (DOI) PET detector module", *IEEE Trans. Nucl. Sci.*, vol. 45, no. 3, pp. 1069-1073, June 1998.

[2] V. Astakhov, P. Gumplinger, C. Moisan, T. J. Ruth, and V. Sossi "Effect of Depth of Interaction Decoding on Resolution in PET: A Simulation Study", *IEEE Trans. Nucl. Sci.*, vol. 50, no. 5, pp. 1373-1378, October 2003.

[3] A. Saoudi, and R. Lecomte, "A novel APD-based detector module for multi-modality PET/SPECT/CT scanners", *IEEE Trans. Nucl. Sci.*, vol. 46, no. 3, pp. 479-484, June 1999.

[4] M. Streun, G. Brandenburg, H. Larue, H. Saleh, E. Zimmermann, K. Ziemons, and H. Halling, "Pulse shape discrimination of LSO and LuYAP scintillators for depth of interaction detection in PET", *IEEE Trans. Nucl. Sci.*, vol. 50, no. 3, pp. 344-347, June 2003.

[5] J. Seidel, J. J. Vaquero, S. Siegel, W. R. Gandler, and M. V. Green, "Depth identification accuracy of a three layer phoswich PET detector module", *IEEE Trans. Nucl. Sci.*, vol. 46, no. 3, pp. 485-490, June 1999.

[6] J.-B. Michaud, R. Fontaine, R. Lecomte, "ARMAX model and recursive least-squares identification for DOI measurement in PET". *IEEE Nuclear Science Symposium Conference Record*, vol. 4, pp. 2386-2390, October 2003.

[7] R. Fontaine, F. Bélanger, N. Viscogliosi, H. Semmaoui, M.-A. Tétrault, J.-B. Michaud, C.M. Pepin, J. Cadorette, and R. Lecomte, "The hardware and signal processing architecture of LabPET^{tm}, a small animal APD-based digital PET scanner", *IEEE Trans. Nucl. Sci.*, vol. 56, no. 1, pp. 3-9, February 2009.

[8] H.C. Yousefzadeh, N. Viscogliosi, M.-A. Tetrault, C.M. Pepin, P. Berard, M. Bergeron, et al., "A fast crystal identification algorithm applied to the LabPET^{tm} phoswich detectors", *IEEE Trans. Nucl. Sci.,* vol. 55, no. 3, pp. 1644-1651, June 2008.

[9] G.F. Knoll, Radiation Detection and Measurement, 3rd ed., 1999.

[10] R. Lecomte, C. M. Pepin, M. D. Lepage, J.-F. Pratte, H. Dautet, and D. M. Binkley, "Performance analysis of phoswich/APD detectors and low-noise CMOS preamplifiers for high-resolution PET systems", *IEEE Trans. Nucl. Sci.*, vol. 48, no. 3, pp. ??-??, June 2001.

[11] M.E. Casey, C. Reynolds, D.M. Binkley, and J.M. Rochelle, "Analysis of timing performance for an APD-LSO scintillation detector", *Nucl. Instrum. Meth. Phys. Res. A*, vol. 504, pp. 143-148, 2003.